Performance of the ATLAS electromagnetic calorimeter under beam tests

F. Hubaut

Performance of the ATLAS electromagnetic calorimeter under beam tests

Fabrice Hubaut [a] *

[a]CPPM, CNRS/IN2P3, Univ. Méditerranée, Marseille, France

The physics program at LHC is highly demanding in terms of detector performance. In particular, the ATLAS electromagnetic calorimeter has to match challenging requirements for energy, position and time resolutions. Calorimeter prototype and production modules have been tested under electron beams at CERN during the last three years. Results are presented and compared to ATLAS requirements.

ATL-CONF-2003-004
07 July 2003

1. Introduction

The ATLAS (A Toroidal LHC ApparatuS) experiment [1], presently under construction, will start operation in 2007 at the LHC [2] proton-proton collider at CERN. This multi-purpose detector has a wide physics program, spanning from precision measurements of $W^{\pm}$ bosons, top and bottom quarks properties, to Higgs boson or supersymmetric particle searches. In most cases, the electromagnetic (EM) calorimeter will play a key role in measuring energy, position and time of electrons and photons.

2. General layout of the ATLAS electromagnetic calorimeter

The LHC extreme operating conditions impose severe constraints on detectors, in terms of radiation tolerance, background rejection capability, noise handling, response speed, spatial coverage and time stability. The EM calorimeter is a lead-liquid argon (LAr) sampling calorimeter with an accordion geometry [3], that guarantees a full azimuthal coverage. It is divided in one barrel ($|\eta| < 1.475$) and two end-caps ($1.375 < |\eta| < 3.2$) and is segmented in depth in three compartments (see figure 1). The sampling 1 (front) is made of narrow strips and performs precise position measurements and γ/π^0 separation. The sampling 2 (middle) has a depth of 16 to 18 X_0 and collects most of the e/γ shower energy. The sampling 3 (back) recovers high energy tails and helps to separate hadronic to electromagnetic particles. In addition, a thin presampler detector corrects energy losses in the upstream material for $|\eta| < 1.8$. In total, almost 200,000 read-out channels give the detector a high granularity. Liquid argon has been chosen for its intrinsic linear behavior, response stability and radiation tolerance. For ease of construction, the barrel part is divided in 32 modules and each end-cap wheel is made of 8 modules. The construction, test and integration of these modules are presently well advanced, and are detailed in a separate contribution [4] within this publication.

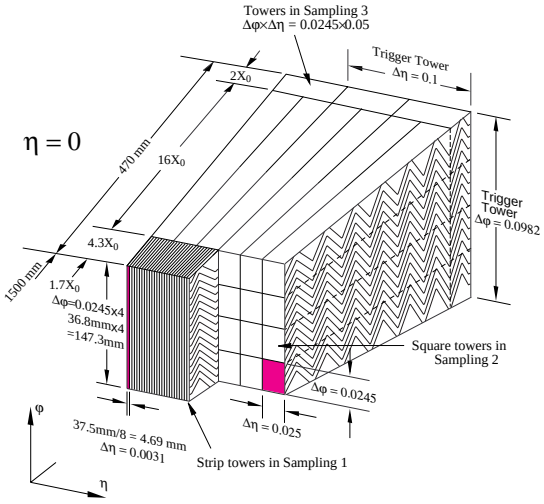

Figure 1. Sketch of the accordion structure and sampling segmentation of the EM calorimeter.

*On behalf of the ATLAS liquid argon group.

3. Performance requirements

The EM calorimeter performance needed to achieve the ATLAS physics goals has been tuned on a few simulated benchmark channels [5], such as H→ $\gamma\gamma$, H→eeee, or heavy gauge bosons, W' and Z', decays. These benchmark channels have guided the design choices described in section 2.

The **energy resolution** can be parametrized as:

$$\frac{\sigma_E}{E} = \frac{a}{\sqrt{E}} \oplus \frac{n}{E} \oplus c \qquad (1)$$

$a/\sqrt{E}$ is the stochastic or sampling term due to statistical fluctuations in the shower development. n is the electronic noise and pile-up contribution. c is the constant term that accounts for all detector imperfections and calibration imprecisions. A 1% resolution on the low mass Higgs ($m_H \lesssim 150$ GeV) implies a stochastic term below $10\%/\sqrt{E(GeV)}$ and a constant term smaller than 0.7% over $0 < |\eta| < 2.5$. The latter term is the most critical issue. It is addressed by a good uniformity in the geometry, a precise calibration system to get 0.5% local constant terms over limited regions of size $\Delta\eta \times \Delta\Phi = 0.2 \times 0.4$, and a cross-calibration of these regions based on $Z^0 \to e^+e^-$ decay signals.

The **angular resolution** on the shower direction should scale as $50\ \text{mrad}/\sqrt{E(GeV)}$, to ensure a low contribution to the $\gamma\gamma$ invariant mass resolution for low mass Higgs search.

The **time resolution** should be around 100 ps for background rejection and for the identification of some decay modes with non-pointing photons.

4. Calibration and signal reconstruction

Each read-out channel is calibrated independently by injecting precise (0.2% accuracy) exponential current pulses, that mimic the triangular ionization signal. This allows to measure its gain and non-linearity. Output signals are amplified, shaped, sampled every 25 ns and then digitized.

The amplitude A of the ionization signal and its arrival time τ are reconstructed as linear combinations of the five samples S_i located around the peak, using the optimal filtering technique [6]:

$$A = \sum_{i=1}^{5} a_i S_i \qquad A \cdot \tau = \sum_{i=1}^{5} b_i S_i \qquad (2)$$

The coefficients a_i and b_i are calculated to minimize the noise and pile-up contribution. They are determined from the noise autocorrelation matrix and the physics signal waveform. The latter is predicted, using the known calibration pulse shape corrected for the different input currents (triangle/exponential) and the different injection points. The level of this prediction is better than 1% on the whole pulse and is around 0.4% at the peak location (see figure 2).

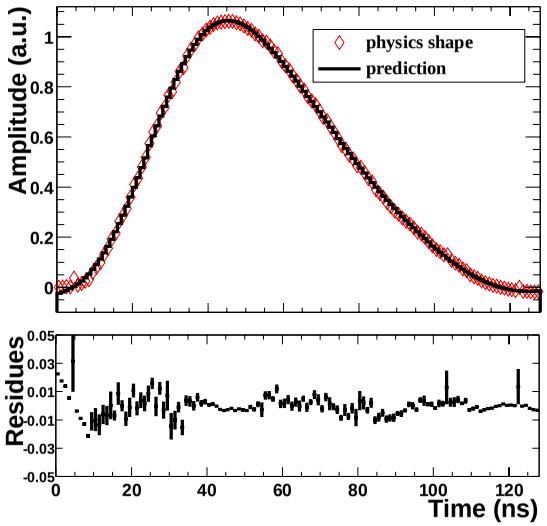

Figure 2. Physics pulse shape prediction (top) and corresponding residues (bottom).

5. Electron reconstruction

As the EM shower is not contained in one read-out cell, the energy is measured in each compartment in a cluster of cells built around the most

energetic one. In order to compensate for energy losses in front of the calorimeter and leakage beyond it, weights are applied to the presampler and the back compartment responses. Moreover, the finite size of the cluster causes a lateral leakage affecting the energy measurement at a level below 0.4%, and the accordion geometry induces a modulation along Φ with similar magnitude. In addition, the specific setting of the high voltage by finite sectors in the end-cap induces a linear variation of the energy response as a function of η in each sector. Finally, unlike in ATLAS, beam test particle arrival times are asynchronous with respect to the 40 MHz clock, and the energy measurement is sensitive to this phase. All these effects are found in good agreement with simulations and have been corrected for.

6. Beam test results

The performance of the EM calorimeter has been extensively tested under electron beams using two full-size prototype modules (one for the barrel and one for the end-cap) and seven production modules (four barrel and three end-cap). An ATLAS-like electronics was used. Results from prototype modules, including noise, cross-talk, time stability, temperature effect, response to muons, γ/π^0 separation, are extensively described in [7,8]. They allowed to improve calorimeter performance. The following results have been obtained with production modules and are similar for all tested modules.

6.1. Energy resolution and uniformity

Energy scans from 10 to 245 GeV have been performed at several positions. After unfolding noise and beam energy uncertainty, the sampling term a is found below $10\%\sqrt{GeV}$ (resp. 12.5) for every barrel (resp. end-cap) positions, whereas the local constant term c is everywhere smaller than 0.4%. This is in good agreement with ATLAS specifications (section 3). The linearity is found to be better than $\pm 1\%$.

To estimate the global constant term of equation (1), the local constant term has to be added quadratically with the response non-uniformity. The latter has been determined by performing position scans through every module cells. As a result, the response non-uniformity is lower than 0.6% on the whole module for the barrel and the end-cap (see figure 3). It is smaller than 0.5% in regions of size $\Delta\eta \times \Delta\Phi = 0.2 \times 0.4$. As required, the resulting global constant term is below 0.7%.

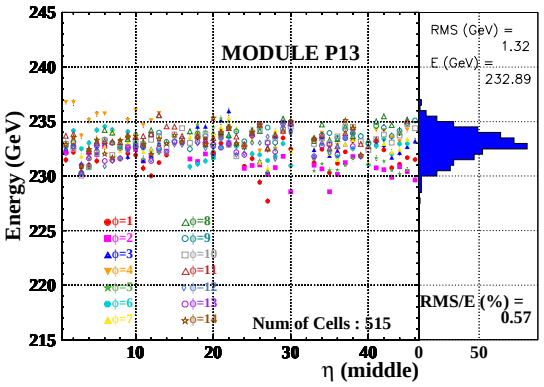

(a)

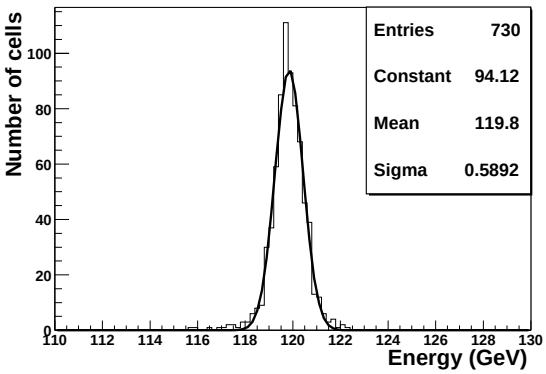

(b)

Figure 3. Response uniformity of (a) a barrel and (b) an end-cap production module.

6.2. Position measurement resolution

Energy-weighted barycenters are calculated in the front and/or in the middle compartments to perform position measurements. In the η direction, corrections for finite cell size are done and the beam chambers resolution is unfolded. The position resolution in the front (resp. middle) section is stable along η and amounts to $0.15 \cdot 10^{-3}$ η-units (resp. $0.35 \cdot 10^{-3}$). These two η measurements can be combined with the longitudinal shower barycenters to estimate the shower direction. An average preliminary 50 mrad/$\sqrt{E(GeV)}$ resolution is achieved over the whole calorimeter which is in agreement with simulations and within ATLAS specifications.

6.3. Time measurement resolution

The optimal filtering technique provides information on the particle arrival time (equation (2)). Cell to cell time differences are studied. Figure 4 shows the results obtained for one barrel cell and its neighbors, as a function of the energy. They are in agreement with the expected electronics contribution. The time resolution amounts to $\sim$ 70 ps at 70 GeV, which is within ATLAS specifications.

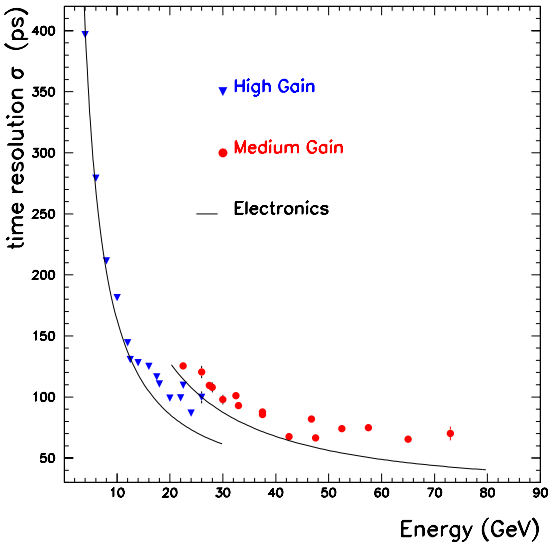

Figure 4. Time resolution (symbols) as a function of the energy, and expected electronics contribution (line).

7. Conclusions and outlook

The several beam tests performed on prototype and production modules show that the ATLAS EM calorimeter meets the physics specifications. The construction, test and integration of the final modules are presently well proceeding [4]. Combined runs of a full barrel wedge and of all end-cap liquid argon calorimeters will take place next year, and will provide a first glimpse of the ATLAS detector.

Acknowledgment

I thank my ATLAS-Larg-EM colleagues for providing me with figures and results. I am indebted to E. Monnier, P. Pralavorio and L. Serin for discussions in the preparation of the talk and the manuscript.

REFERENCES

1. The ATLAS Technical Proposal, CERN/LHCC/94-43 (1994).
2. The Large Hadron Collider, CERN/AC/95-05 (1995).
3. ATLAS Liquid Argon Calorimeter, Technical Design Report, CERN/LHCC/96-41 (1996).
4. A. Jérémie, The ATLAS liquid argon electromagnetic calorimeter construction status, these proceedings.
5. ATLAS Calorimeter Performance, Technical Design Report, CERN/LHCC/96-40 (1996).
6. W.E. Cleland, E.G. Stern, Nucl. Inst. Meth. A338 (1994) 467.
7. ATLAS Electromagnetic Liquid Argon Calorimeter Group, Performance of the ATLAS electromagnetic calorimeter barrel module 0, Nucl. Inst. Meth. A500 (2003) 202.
8. ATLAS Electromagnetic Liquid Argon Calorimeter Group, Performance of the ATLAS electromagnetic calorimeter end-cap module 0, Nucl. Inst. Meth. A500 (2003) 178.